NUCL SCI TECH (2018) 29:113
https://doi.org/10.1007/s41365-018-0445-6

Bunch-by-bunch longitudinal phase monitor at SSRF

Yi-Mei Zhou[1,2] · Han-Jiao Chen[1,2] · Shan-Shan Cao[1,2] · Yong-Bin Leng[1,2]

Received: 16 January 2018 / Revised: 19 March 2018 / Accepted: 10 April 2018 / Published online: 4 July 2018

Abstract Beam signals captured from a button-type pickup contain multidimensional information including the bunch charge, transverse position, bunch length, and longitudinal phase. A bunch phase monitor, which retrieves longitudinal phase information from a pickup signal at a bunch-by-bunch rate, has been developed at the Shanghai Synchrotron Radiation Facility. This paper introduces the basic principles, system setup, data processing method, and preliminary experimental results of this system. The systematic measurement error introduced by the limited system bandwidth, bunch length, and bunch charge variation was studied using simulation data. The random measurement uncertainty was evaluated using experimental beam data. The experimental result shows that the longitudinal phase resolution of this system is better than 1.0 ps. The first application, measuring the relationship between the longitudinal phase and bunch charge to determine the energy loss factor, was implemented, and the preliminary result is also discussed.

Keywords Bunch-by-bunch · Longitudinal phase · Resolution · Pickup signal · Software resampling

This work was supported by the National Natural Science Foundation of China (Nos. 11575282, 11375255).

✉ Yong-Bin Leng
lengyongbin@sinap.ac.cn

1 Shanghai Institute of Applied Physics, Chinese Academy of Sciences, Shanghai 201800, China

2 Shanghai Synchrotron Radiation Facility, Chinese Academy of Sciences, Shanghai 201204, China

1 Introduction

The Shanghai Synchrotron Radiation Facility (SSRF), which consists of a 150 MeV linear accelerator, a 180 m, 3.5 GeV booster, and a 432 m, 3.5 GeV storage ring, is a multi-bunch, high-energy third-generation light source [1]. The harmonic number is 720 at a radio frequency (RF) of 499.654 MHz. To improve the efficiency and quality of the light, a top-up filling pattern was adopted at the end of 2012, which results in more frequent beam injections and storage of approximately 500 bunches with a 2 ns spacing. The multi-bunch operating mode makes bunch-by-bunch beam diagnosis necessary. Owing to the addition of new insertion devices (IDs), the beam impedance has become an important parameter for the study of the longitudinal dynamics.

Beam position monitors (BPMs) are in wide use in modern light sources and are used in daily operation and machine studies. At the SSRF, there are a total of 140 BPMs around the storage ring, including 40 high-resolution BPMs at the entrance or exit of drift spaces and 100 regular BPMs in the bending areas [2]. Information on the bunch charge, transverse position, and longitudinal phase is contained in the button BPM signals. Through a high-speed oscilloscope, the BPM signals can be measured directly to obtain multidimensional information.

The longitudinal phase is usually detected from the phase difference between a beam pulse and a reference frequency signal. The longitudinal phase was once measured using a phase detector [3], a commercial Libera unit [4], and a frequency mixing technique [5]. Studies on the energy loss and resistive impedance related to the synchronous phase shift have also been performed at Laboratório Nacional de Luz Síncrotron [6]. However, all of these methods yielded averaged phase measurements and neglected the effect of the finite bunch length. Another method of selecting a specific bunch in a bunch train using a high-speed gate has been used at KEKB [7]. A bunch phase monitor based on this method was designed to measure the bunch-by-bunch phase shift at the SSRF. Compared with the method at KEKB, bunch-by-bunch phase measurement allows the execution of signal processing over each bunch period with precise results.

In the following sections, a basic expression of the button BPM signal with the longitudinal phase is derived in Sect. 2. The experimental hardware and off-line data processing method of the bunch phase monitor are described in Sect. 3. Test results are presented in Sect. 4, and an application involving the relationship between the longitudinal phase and bunch charge is presented in Sect. 5.

2 Theoretical descriptions

To achieve three-dimensional (3D) position measurement, the transverse position of the button electrode in the SSRF storage ring has been measured [8]. However, to study the multi-bunch instability, transverse position measurement alone is not sufficient. Thus, we conducted bunch-by-bunch measurement of the longitudinal phase in this study. The transfer function of the BPM signal indicating the transverse position and longitudinal phase is derived in this section.

A cross section of the operating button BPMs is shown in Fig. 1. A line charge at the position (δ, θ) within the probe radius a and pipe radius b.

In the following analysis [9], we consider N particles of charge e in a bunch of rms temporal length σ (in time units). When a Gaussian bunch shape was used, the time-domain expression of a single bunch could be obtained using t_0, which is the phase difference relative to the RF clock.

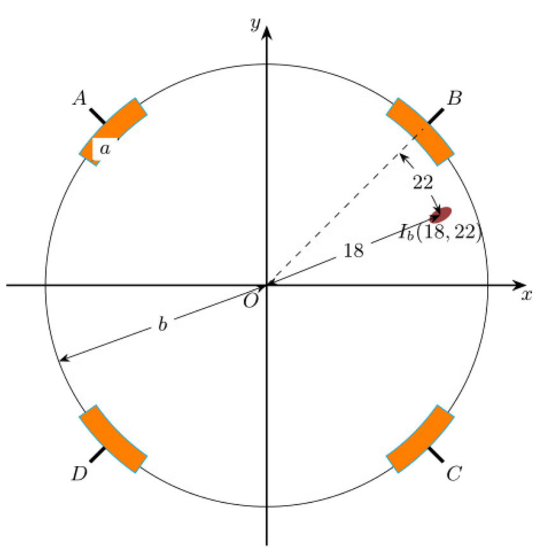

Fig. 1 (Color online) Cross section of button-type BPM

$$I_0(t) = \frac{eN}{\sqrt{2\pi}\sigma}\exp\left(-\frac{(t-t_0)^2}{2\sigma^2}\right). \tag{1}$$

When the bunch position and phase information were calculated, the image charge method was used. The image charge on a button is given by [10]

$$Q(t) = \frac{\text{Button area}}{\text{Duct circumference}} \cdot I(t) \cdot F(\delta, \theta). \tag{2}$$

Then the image current out of the button is given by

$$I_{\text{img}} = \frac{\mathrm{d}Q}{\mathrm{d}t} = \frac{\pi a^2}{2\pi b} \cdot \frac{1}{\beta c} \cdot \frac{\mathrm{d}I}{\mathrm{d}t} \cdot F(\delta, \theta). \tag{3}$$

The button voltage is the product of the current out of the button and the impedance seen by this current. When the impedance is Z, the signal voltage can be expressed as

$$V_{\text{b}}(t) = -\frac{\pi a^2 Z}{2\pi b \beta c} \cdot \frac{t-t_0}{\sigma^2} \cdot I_0(t) \cdot F(\delta, \theta), \tag{4}$$

where the position related equation has been derived in Ref. [11]:

$$F(\delta, \theta) = \frac{a^2 - \delta^2}{a^2 + \delta^2 - 2a\delta\cos\theta}, \tag{5}$$

$$\delta = \sqrt{x^2 + y^2}, \tag{6}$$

$$\theta_{A,B,C,D} = \frac{m\pi}{4} - \tan^{-1}\left(\frac{y}{x}\right) \qquad (m = 3, 1, 7, 5). \tag{7}$$

Equation (4) shows that when the geometry of the pickup is definite, the induced voltages on the electrodes are related to the beam current I_0, bunch length σ, transverse position $F(\delta, \theta)$, and longitudinal phase t_0.

The work specifies some of the parameters of our accelerator, which are shown in Table 1.

Table 1 Parameters of the SSRF storage ring

Parameters	Values
Energy, E (GeV)	3
Button radius, a (mm)	5
Duct radius, b (mm)	17.5
Beam current, I_0 (mA)	260
RF, f_{rf} (MHz)	499.654
Harmonic number, h	720
Bunch length, σ (ps)	18
Synchronous phase, Φ_0 (°)	71.9

According to the theoretical analysis above, the limited bandwidth of the BPM probe will introduce time delays, which will result in systematic measurement errors. The zero-crossing point of the button pickup signal corresponds to the peak point of the input Gaussian signal if the time delay is ignored, as shown in Fig. 2. However, different bunch lengths will result in different time delays. Whether the measurement error caused by this shift can be ignored will be discussed below.

3 System setup and data processing

The system frame of the 3D BPM is shown in Fig. 3. A broadband oscilloscope with a 25 GHz maximum sampling rate and 6 GHz analog bandwidth is employed for our experiment owing to its high-sampling rate and available memory capacity (10 M samples, 276 turns of the SSRF operating mode). To reduce the signal noise, internal digital low-pass filters (LPFs) in the oscilloscope offer a convenient method of signal optimization, and we choose five different filters for the oscilloscope, as shown in Fig. 3.

If the sampling rate is equal to the machine RF (synchronized sampling), the peak of the raw data can be used to calculate the bunch charge and bunch position (Δ over Σ method) by the transverse position measurement subsystem, all of which have been measured at SSRF [13]. In this study, the bunch-by-bunch phase was measured by the bunch phase measurement subsystem using the zero-crossing detection method. For the SSRF, however, the RF usually varies between 499.654 and 499.674 MHz depending on the ground temperature. Because the frequency of the real signal does not match the internal clock of the oscilloscope, a software resampling algorithm [14] is used to pick up each zero-crossing point on the basis of the real period T_{rf}.

By using the correct sampling frequency and initial sampling phase, synchronizing sampled data can be calculated using the spline interpolation method. The off-line data processing schematic shows how the bunch phase and position information are captured from the oscilloscope by a process that includes software resampling, spline interpolation, and zero-crossing detection. The data points used to calculate the bunch position and phase are shown in Fig. 4. The peak voltages (stars) were interpolated to measure the transverse position, and the circles, which represent the measured results around the zero-crossing points, were used to measure the longitudinal phase.

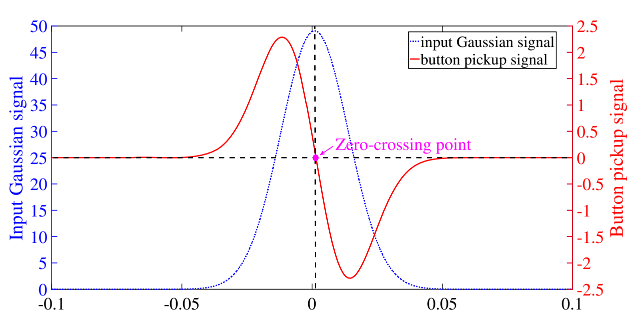

Fig. 2 (Color online) Ideal button pickup signal induced by a Gaussian beam

The system bandwidth is a very important characteristic that influences the measurement uncertainty and systematic error. The bandwidth selection of the internal digital LPFs in the oscilloscope is crucial to the systematic error measurement because the waveforms of signals sampled under different bandwidths are different. The first requirement for bandwidth selection is that there is no crosstalk between bunches. Second, using more sampling points can improve the precision of the zero-crossing detection method, and four sampling points at the rising edge are chosen in our experiment. Finally, once the above conditions are met, we need to choose as wide a bandwidth as possible.

Owing to the limited bandwidth of the BPM probe and the low-pass characteristics of the signal transmission cable, we need to choose a suitable LPF bandwidth to obtain better phase measurement resolution. Figure 5 shows the original waveforms of signals sampled under different bandwidths. At bandwidths of 6 and 4 GHz, the number of sampling points was not sufficient to measure the bunch phase, and the points obtained at a bandwidth of 4 GHz bandwidth did not exhibit a linear relationship.

The advantages of a wide bandwidth are that the signal slope is steeper at the zero-crossing points and the measurement resolution is better. The disadvantages are the delayed beam arrival time and the separation of the beams, as a result of which our acquisition system cannot obtain enough sampling points.

In addition, to estimate the relationship between the phase measurement error and bunch length, simulations with different bunch lengths (13–25 ps) were performed using CST software. The original phase shift at the zero-crossing point of the button pickup was 7 ps. When the pickup signal was filtered by a digital LPF, the waveform and phase deviation changed, as shown in Fig. 6. The relationship between the bunch length and phase of LPFs with different bandwidths is shown in Fig. 7. It can be seen that the phase shift decreased to 4 ps when the bandwidth of the LPF was 3 GHz, introducing a 3 ps phase error relative to the original measurement. The result is very small and can be neglected in most applications of our apparatus. However, the practical measured bunch length of the SSRF (18–20 ps) is smaller than the simulation values [12]. Thus, the phase measurement error caused by the bunch length can be neglected in the following random

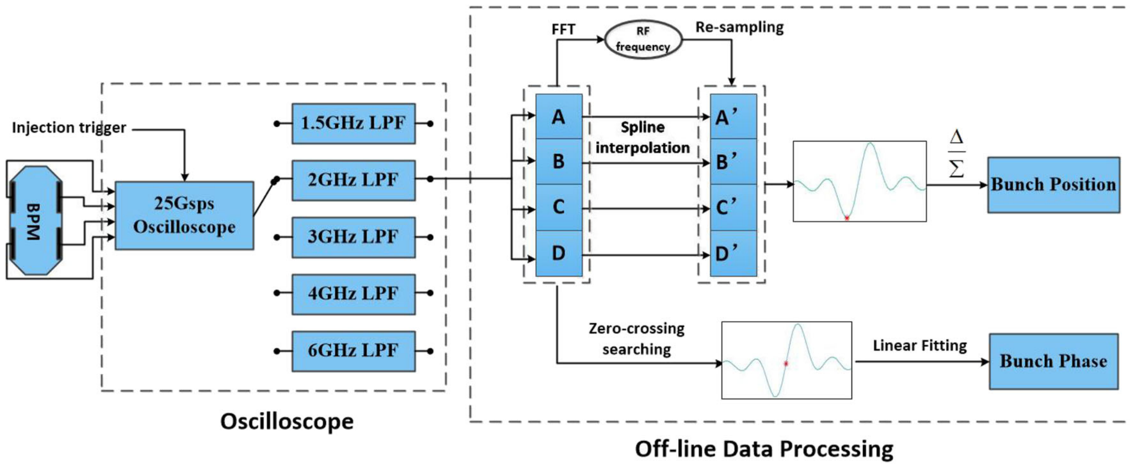

Fig. 3 (Color online) System frame of the 3D BPM

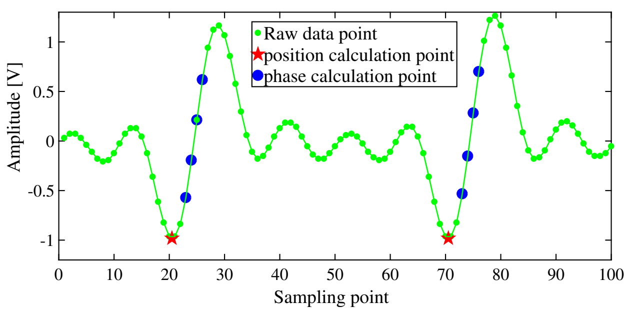

Fig. 4 (Color online) Diagram of data points used in position and phase calculation

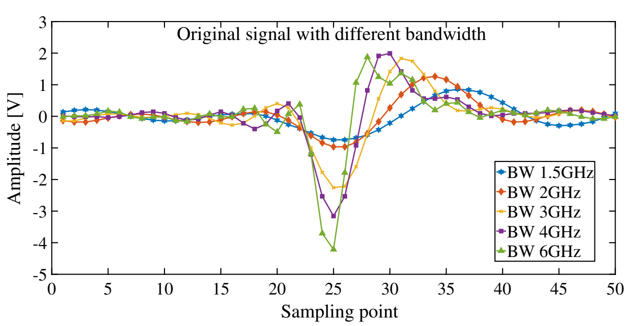

Fig. 5 (Color online) Signals sampled under different bandwidths

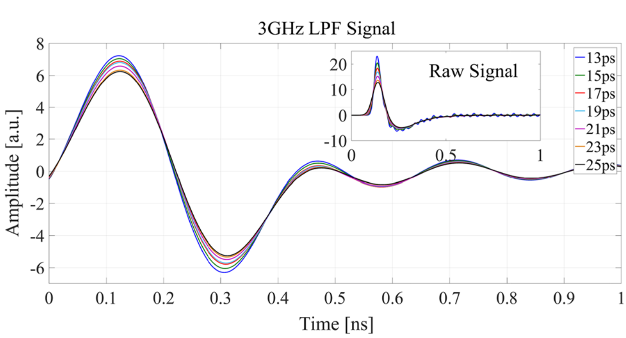

Fig. 6 (Color online) Low-pass-filtered signal at 3 GHz bandwidth

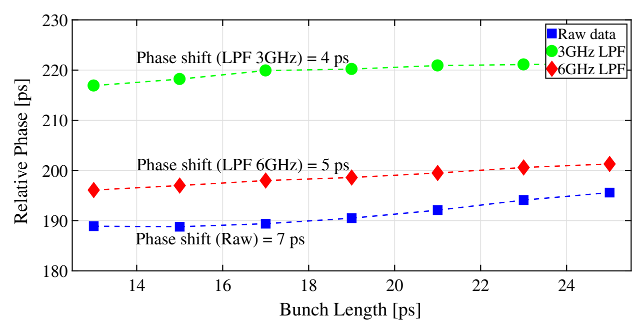

Fig. 7 (Color online) Relationship between bunch length and phase under LPFs with different bandwidths

measurement uncertainty evaluation. Therefore, the longitudinal phase can be measured by linear fitting at the zero-crossing points, and we measured the intercept with the timeline.

Considering the limited system bandwidth, bunch charge variation, and bunch length discussed in this section, we chose 3 GHz as the LPF bandwidth.

4 Performance evaluation

The resolution is a particularly important parameter for evaluating the random measurement uncertainty. In steady-state operation, the bunches oscillate at the same frequency and amplitude, resulting in a fixed phase shift between two adjacent bunches. If we consider the balanced bunch acceleration phase and the systematic errors, the phase equation can be written as $\Phi_i(t)$ and $\Phi_j(t)$:

$$\Phi_i(t) = \Phi_{i0} + n_i, \tag{8}$$

$$\Phi_j(t) = \Phi_{j0} + n_j. \tag{9}$$

However, for the same system and the same bunch charge, the phase measurement uncertainty can be obtained by the following formula because the balanced bunch acceleration phase and the systematic error are the same ($\Phi_{i0} = \Phi_{j0}$, $n_i = n_j$).

$$Rms = \mathrm{std}(\Phi_i(t) - \Phi_j(t))/\sqrt{(2)}. \tag{10}$$

To evaluate the measurement uncertainty for different bunch charges, a dedicated beam experiment with a special fill pattern (shown in Fig. 8) was performed. In this experiment, six groups of bunches were filled, where each group contained two equal-charge bunches.

For example, for bunches 1 and 101, the longitudinal phase can be measured separately using the zero-crossing detection method described earlier (as shown in Fig. 9). Then the phase resolution can be found using Eq. 10; a histogram of the phase difference of the two bunches is shown in Fig. 10. A comparison of the six experimental results shows that the best longitudinal phase resolution of this system was 1 ps at 2 nC. At the same time, we can obtain the relationship between the phase resolution and bunch charge according to the experimental results, as shown in Fig. 11. When the bunch charge is higher, a better phase resolution can be obtained.

5 Application

The parasitic mode energy loss due to interaction of the beam with the resistive impedance of the vacuum chamber and IDs is an important parameter for the longitudinal dynamics. The parasitic mode loss factor (k) is proportional to the dependence of the longitudinal phase and bunch charge, which is defined as the slope coefficient (K). Because the phase measurement system measures the bunch-by-bunch phase directly, it is easy to study the relationship between the longitudinal phase and bunch charge. The correlation formula is

$$k = \frac{\Delta\phi}{eN} V_{\mathrm{rf}} \sin\phi_0, \tag{11}$$

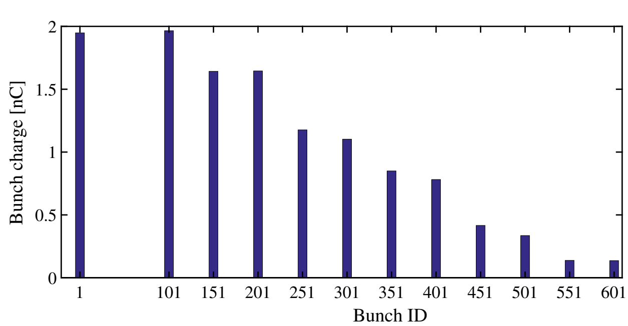

Fig. 8 (Color online) Diagram of special filling pattern

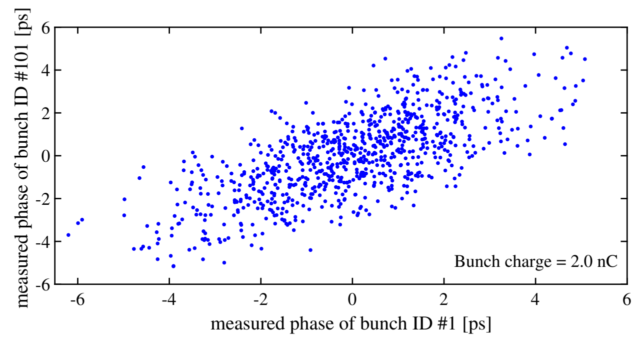

Fig. 9 (Color online) Phase correlation between two bunches at 2 nC

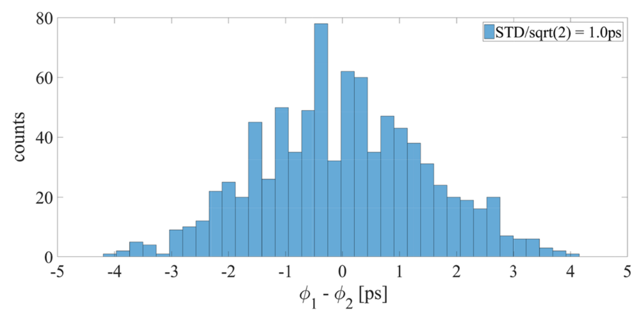

Fig. 10 (Color online) Histogram of the phase difference of the two bunches

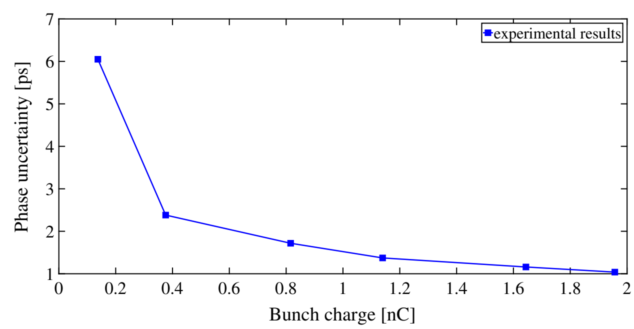

Fig. 11 (Color online) Relationship between phase resolution and bunch charge

where $Q = eN$, and V_{rf} is the RF cavity voltage. The measured phase $\Delta\phi$ is the phase shift relative to the synchronous phase.

To evaluate the relationship between the bunch phase and charge, we repeated multiple sets of experiments under the same conditions using the phase measurement system in user operation. During daily operation, the ring was filled with four bunch trains with a total beam current of 260 mA (as shown in Fig. 12). The bunch phase and charge were calculated using the method described above, and the experimental results are shown in Fig. 13. It can be concluded that the longitudinal phase is linear with respect to the bunch charge. The slope coefficient was evaluated within a certain error range, and its value was

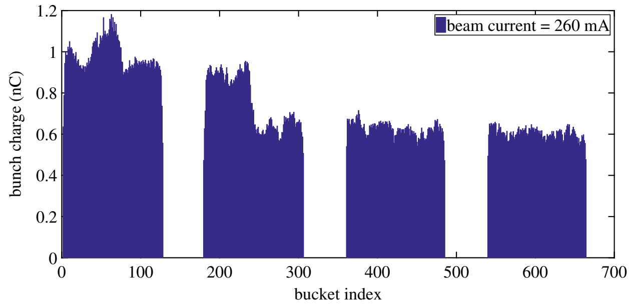

Fig. 12 (Color online) Top-up filling pattern

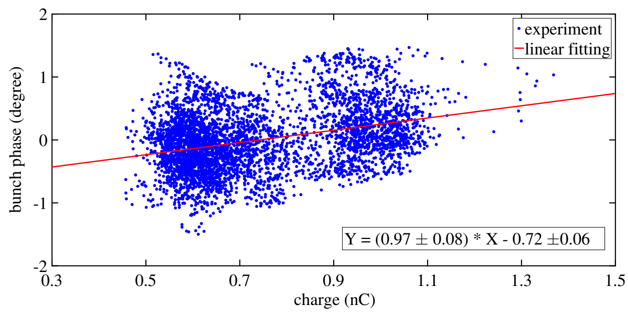

Fig. 13 (Color online) Relationship between bunch charge and longitudinal phase

approximately 1 °/nC. Measurement of the relationship between the longitudinal phase and bunch charge is helpful for future research on the impedance and other related issues.

6 Summary

A phase monitor based on a high-sampling-rate oscilloscope was successfully implemented at the SSRF. The systematic measurement error due to the button electrode response at different bunch lengths was evaluated with a phase shift of several picoseconds, which is relatively small and can be neglected in most applications of our facility. To achieve the best performance, beam signals with different bandwidths were captured and analyzed to evaluate the time-domain data processing method. Finally, 3 GHz was selected as the most suitable LPF bandwidth. The phase resolution for different bunch charges was also validated, and the best resolution was 1.0 ps at 2 nC.

Compared to previous methods, this system can directly measure the phase of each bunch in every period term. Therefore, it can easily be used to study the dependence of the longitudinal phase and bunch charge, which was in line with a linear relationship.

Furthermore, bunch-by-bunch phase measurement can be used to observe the beam instability during the transient injection process. It is useful for next-generation synchrotron radiation and for future research on new injection methods.

References

1. H.H. Li, G.M. Liu, W.Z. Zhang, et al., Beam dynamics in the SSRF storage ring, in *Proceeding of the 1st international particle accelerator conference*, (JACoW, Kyoto, Japan, 2010), pp. 2591–2593
2. Y.B. Leng, W.M. Zhou, R.X. Yuan et al., Beam position monitor system for SSRF storage ring. Nucl. Tech. **33**, 401–404 (2010)
3. T. Ohshima, A. Yamashita, M. Yoshioka, Beam phase measurement of stored bunch, in *Proceeding of the 10th European particle accelerator conference*, (JACoW, Edinburgh, UK, 2006), pp. 1133–1135
4. K. Scheidt, B. Joly, Upgrade of beam phase monitors for the ESRF injector and storage ring, in *Proceeding of the 2nd international beam instrumentation conference*, (JACoW, Geneva, Switzerland, 2013), pp. 757–760
5. W.K. Lau, S.J. Lin, M.S. Yeh et al., Development of a digital longitudinal damper for the TLS storage ring. Part. Accel. Conf. **2**, 2377–2379 (1997). https://doi.org/10.1109/PAC.1997.751214
6. R.H.A. Farias, L. Liu, A.R.D. Rodrigues et al., Oscilloscope measurement of the synchronous phase shift in an electron storage ring. Phys. Rev. Spec. Top. Accel. Beams **4**, 072801 (2001). https://doi.org/10.1103/PhysRevSTAB.4.072801
7. T. Ieiri, K. Akai, H. Fukuma et al., Bunch-by-bunch measurements of the betatron tune and the synchronous phase and their applications to beam dynamics at KEKB. Phys. Rev. Spec. Top. Accel. Beams **5**, 094402 (2002). https://doi.org/10.1103/PhysRevSTAB.5.094402
8. Z.C. Chen, L.W. Lai, Y.B. Leng, et al., Precise position measurement by analyzing the correlation between electrodes of a single BPM, in *Proceeding of the 6th international particle accelerator conference*, (JACoW, Geneva, Switzerland, 2015), pp. 975–977
9. R.E. Shafer, Beam position monitoring. AIP Conf. Proc. **249**, 601–636 (1992). https://doi.org/10.1063/1.41980
10. S.R. Smith, Beam position monitor engineering. AIP Conf. Proc. **390**, 50–65 (1997). https://doi.org/10.1063/1.52306
11. Y.B Yan, Ph.D. thesis, research of SSRF BPM data acqusition system and preliminary application, Shanghai Institute of Applied Physics, Chinese Academy of Sciences, 10–15 (2009) (**in Chinese**)
12. H.J. Chen, L.W. Duan, Y.B. Leng et al., Bunch-by-bunch beam length measurement using two-frequency system at SSRF, in *Proceeding of the 6th international beam instrumentation conference*, (JACoW, Michigan, USA, 2017) (**in press**)
13. Y.B. Leng, Z.C. Chen, L.W. Lai, et al., Bunch by bunch DBPM processor development and preliminary experiment in SSRF, in *Proceeding of the 6th international particle accelerator conference*, (JACoW, Geneva, Switzerland, 2015), pp. 984–986
14. Y. Yang, Y.B. Leng, Y.B. Lan, N. Zhang, Bunch-by-bunch beam position and charge monitor based on broadband scope in SSRF, in *Proceedings of 4th international particle accelerator conference*, (JACoW, Shanghai, China, 2013), pp. 595–597